

Original Article

Shenmai injection enhances the cytotoxicity of chemotherapeutic drugs against colorectal cancers via improving their subcellular distribution

Wen-yue LIU^{1, #}, Jing-wei ZHANG^{1, #}, Xue-quan YAO², Chao JIANG², Ji-chao HE¹, Pin NI¹, Jia-li LIU¹, Qian-ying CHEN¹, Qing-ran LI¹, Xiao-jie ZANG¹, Lan YAO¹, Ya-zhong LIU¹, Mu-lan WANG³, Pei-qiang SHEN³, Guang-ji WANG^{1, *}, Fang ZHOU^{1, *}

¹Key Laboratory of Drug Metabolism and Pharmacokinetics, State Key Laboratory of Natural Medicines, China Pharmaceutical University, Nanjing 210009, China; ²Department of Digestive Tumor Surgery, Affiliated Hospital of Nanjing University of Chinese Medicine, Nanjing 210009, China; ³Chiatai QingChunbao Pharmaceutical Co Ltd, Hangzhou 310023, China

Abstract

Shenmai injection (SMI) is a Chinese patent-protected injection, which was mainly made of Red Ginseng and Radix Ophiopogonis and widely used for treating coronary heart disease and tumors by boosting Qi and nourishing Yin. In this study we examined whether SMI could produce direct synergetic effects on the cytotoxicity of adriamycin (ADR) and paclitaxel (PTX) in colorectal cancers *in vivo* and *in vitro*, and explored the underlying pharmacokinetic mechanisms. BALB/c nude mice with LoVo colon cancer xenografts were intraperitoneally injected with ADR (2 mg·kg⁻¹·3d⁻¹) or PTX (7.5 mg·kg⁻¹·3d⁻¹) with or without SMI (0.01 mL·g⁻¹·d⁻¹) for 13 d. Co-administration of SMI significantly enhanced the chemotherapeutic efficacy of ADR and PTX, whereas administration of SMI alone at the given dosage did not produce visible anti-cancer effects. The chemosensitizing action of SMI was associated with increased concentrations of ADR and PTX in the plasma and tumors. In Caco-2 and LoVo cells *in vitro*, co-treatment with SMI (2 μL/mL) significantly enhanced the cytotoxicity of ADR and PTX, and resulted in some favorable pharmacokinetic changes in the subcellular distribution of ADR and PTX. In addition, SMI-induced intracellular accumulation of ADR was closely correlated with the increased expression levels of P-glycoprotein in 4 colon cancer cell lines ($r^2=+0.8558$). SMI enhances the anti-cancer effects of ADR and PTX in colon cancers *in vivo* and *in vitro* by improving the subcellular distributions of ADR and PTX.

Keywords: traditional Chinese medicine; Shenmai injection; colorectal cancers; adriamycin; paclitaxel; chemosensitization; pharmacokinetics; P-glycoprotein

Acta Pharmacologica Sinica (2017) 38: 264–276; doi: 10.1038/aps.2016.99; published online 21 Nov 2016

Introduction

Cancer, a refractory disease that threatens human health, has continued to rise in incidence over the past decade. Although some progress has been made in cancer treatment, the recovery rate of patients with malignant tumors is low. Clinical observations have shown that good therapeutic effects are rare with any single treatment^[1]. For this reason, multidrug therapy is often used in clinical settings to address the ineffectiveness of and resistance to a mono-substance.

As one of the world's largest and most biodiverse regions, China has abundant populations of medical plant species. Traditional Chinese medicine (TCM) is gaining a reputation

as a trove of synergistic therapeutic agents that is suitable for use alongside Western medicine, especially considering their ability to reduce side effects and increase efficacy^[2]. A substantial body of data has demonstrated that TCM can enhance the anti-tumor effects of chemotherapeutics, defined here as enhancing human immunity, inhibiting the growth of cancer cells, and improving hematopoietic function^[3].

Shenmai injection (SMI), which is derived from a traditional Chinese formula called Shenmaisan, mainly consists of Red Ginseng and Radix Ophiopogonis. SMI is commonly used in coronary heart disease and chronic pulmonary heart disease treatment^[4]. Recently, it has been demonstrated that SMI can help increase anti-tumor effects. Zhu^[5] reported that intraperitoneal chemotherapy plus SMI is effective in treating post-operative patients with advanced colorectal cancer. Additionally, SMI has effect-enhancing and toxicity-reducing actions when co-administered with anti-tumor agents for sev-

[#]These authors contributed equally to this work.

^{*}To whom correspondence should be addressed.

E-mail zf1113@163.com (Fang ZHOU);

guangjiwang@hotmail.com (Guang-ji WANG)

Received 2016-04-20 Accepted 2016-08-26

eral malignancy types, including lung cancer^[6], liver cancer^[7], breast cancer^[8] and gastric cancer^[9]. However, most studies have focused on improving the immune function of cancer patients and decreasing the side effects of chemotherapy. There is not sufficient direct evidence to confirm this effect-enhancing phenomenon, and its underlying mechanisms remain unknown.

Pharmacokinetics is the study of drug absorption, distribution, metabolism, and excretion in the body. Drug-metabolizing enzymes and transporters are the main factors that affect pharmacokinetic actions. TCM can affect the expression and functions of both drug-metabolizing enzymes and transporters when combined with Western medicines, changing the efficacy and side effects of the drugs. Recent reports have demonstrated that SMI can inhibit the activities of the hepatic metabolic enzymes CYP3A1/2 and CYP2C6^[10] and that SMI could significantly affect the CYP3A-mediated metabolism of midazolam^[11, 12]. Furthermore, the ginsenoside component of SMI could attenuate the efflux function of P-glycoprotein, reversing multidrug resistance^[13]. The influence of SMI on drug-metabolizing enzymes and transporters suggests that SMI might affect the pharmacokinetic actions of its co-administered drugs.

This paper evaluated the synergistic effect of SMI with adriamycin (ADR) and paclitaxel (PTX) on a colon cancer xenograft model *in vivo* and colon cancer cells *in vitro*. Its mechanisms were also studied based on macro and micro pharmacokinetics. In conclusion, the current study provides both innovative models for adjuvant cancer therapy with traditional Chinese formulae and pre-clinical pharmacokinetic data for the application of this novel form of therapy.

Materials and methods

Materials

Shenmai (injection form) was obtained from Chiatai Qingchunbao Pharmaceutical Co Ltd (Zhejiang, China). Doxorubicin hydrochloride (injection form) was purchased from Zhejiang Hisun Pharmaceutical Co Ltd (Zhejiang, China). Paclitaxel (injection form) was purchased from the Yangtze River Pharmaceutical Group (Jiangsu, China). Azithromycin and docetaxel were purchased from the National Institute for the Control of Pharmaceutical and Biological Products (NICPBP) (Beijing, China).

Animals and treatment

Male athymic BALB/c nude mice with LoVo colon cancer xenografts (9 weeks old, 18–22 g) were purchased from Shanghai Slack Laboratory Animal Co, Ltd (Shanghai, China). The mice were maintained in autoclaved filter-top microisolator cages in a temperature-controlled environment and provided with food and water *ad libitum*. Animal care and surgery protocols were approved by Animal Care Committees of the China Pharmaceutical University. Here, 100 mice were randomly assigned to the following six treatment groups: (a) control group: saline, 0.01 mL·g⁻¹·d⁻¹; (b) SMI group: 0.01 mL·g⁻¹·d⁻¹; (c) ADR group: 2 mg·kg⁻¹·3d⁻¹; (d) ADR+SMI group:

SMI 0.01 mL·g⁻¹·d⁻¹ and ADR 2 mg·kg⁻¹·3d⁻¹; (e) PTX group: 7.5 mg·kg⁻¹·3d⁻¹; and (f) PTX+SMI group: SMI 0.01 mL·g⁻¹·d⁻¹ and PTX 7.5 mg·kg⁻¹·3d⁻¹. Mice in each group were given drugs via intraperitoneal injection.

Xenograft tumor model studies

The mice were weighed, and the (a) major and (b) minor axes were measured daily before administration. The tumor volume (TV) was calculated using the following formula:

$$TV (\text{mm}^3) = 1/2 \times a \times b^2$$

At the end of 2 weeks, the mice were killed and the tumor xenografts were removed and weighed. The inhibitory rate for the tumor weight and volume were calculated using the following formula: Reduction rate = (1 - mean of treatment group / mean of control group) × 100%.

Cell culture

Caco-2 and LoVo cells were obtained from American Type Culture Collection (Rockville, MD, USA). Cells were routinely cultured in DMEM supplemented with 10% fetal bovine serum, 1% nonessential amino acids, 1 mmol/L sodium pyruvate, and 100 U/mL penicillin and streptomycin (Gibco-Invitrogen, USA). P-glycoprotein (P-gp)-overexpression MCF-7/Adr cells derived from parental MCF-7 cells by adriamycin selection were obtained from Institute of Hematology and Blood Diseases Hospital (Tianjin, China) and cultured in RPMI-1640 supplemented with 10% fetal bovine serum and 100 U/mL penicillin and streptomycin (Gibco-Invitrogen, USA). The cells were grown in an atmosphere of 5% CO₂ at 37°C and cell medium was changed every other day. Cells were passaged upon reaching about 80% confluence.

In vitro cytotoxicity assay

Cells were seeded in 96-well plates at a density of 5 × 10³ cells per well. After 24 h of incubation at 37°C with 5% CO₂, old growth medium was removed and cells were incubated for 48 h in 200 μL of medium containing ADR or PTX with or without SMI. Cell survival was measured using tetrazolium salt MTT assay. MTT (20 μL, 5 mg/mL) solution was added to each well. The plate was incubated for an additional 4 h; then, 200 μL of DMSO was added to each well to dissolve any purple formazan crystals that formed. The plates were shaken before the relative color intensity was measured. The absorbance at 570 nm for each well was measured using a microplate reader (BioTek, USA).

Hoechst 33258 staining for apoptotic cells

Apoptosis was detected by assessing nuclear morphology as stained using Hoechst 33258. Caco-2 and LoVo cells were seeded in 12-well plates and cultured at 37°C for 24 h. Cells were then incubated for another 24 h with medium containing reagents. Samples were fixed with 4% paraformaldehyde in PBS for 15 min, stained with 10 μg/mL Hoechst 33258 in PBS at room temperature for 15 min and washed twice with ice-cold PBS. Then, cell monolayers were examined using a fluorescence microscope (Leica).

Annexin V/PI staining

Colon cancer cells were cultured in six-well plates at 1×10^6 cells/well. The cells were then treated with chemotherapeutics alone or in combination with SMI for 24 h. Cells were washed twice with cold PBS and centrifuged; then, 195 μ L of FITC-conjugated annexin V binding buffer and 5 μ L of annexin V-FITC were added. The cells were incubated for 10 min at room temperature in the dark according to the manufacturer's instructions. Next, the samples were analyzed immediately by flow cytometry. For each experiment, the procedures described above were performed three times.

Cellular accumulation of ADR and PTX

Cellular uptake of ADR and PTX was determined in the presence or absence of various SMI concentrations. Caco-2 and LoVo cells were seeded in 24-well plates and grown until they reached 90%–95% confluence. HBSS solutions containing the corresponding reagent were equilibrated at 37°C before use. The medium was removed and cells were washed with 37°C PBS. Then, treatment solutions were added to cells. After 1 h of incubation, the supernatant was removed and cells were washed with ice-cold PBS and frozen in 500 μ L deionized water at -80°C. Then, the plates were unfrozen and cells were lysed with an ultrasonic processor to determine the concentration. The ADR and PTX concentrations were determined by LC-MS/MS, as previously described^[14]. Cellular uptake of chemotherapeutics was calibrated by cellular protein content, which was determined using a BCA Protein Assay Kit (Beyotime, China).

Subcellular localization of chemotherapeutics

Two methods were used to determine the effect of SMI on the subcellular distribution of chemotherapeutics. First, the drug concentration in different cell compartments was determined. The cytoplasm, mitochondria, and nuclei were isolated according to the instructions provided with a KenGen Mitochondria/Nuclei Isolation Kit (Nanjing KeyGen Biotech Co, Ltd, China). The ADR and PTX concentrations in each subcellular compartment were determined by LC-MS/MS and further adjusted to the concentration based on the initial dosing volume. The cytoplasm, mitochondria and nuclear protein contents were determined using a BCA Protein Assay Kit. According to the subcellular localization of the organelles, LC-MS/MS determined the concentration/protein fraction ratio.

In addition, fluorescent dyes were used to observe cell organelles and drugs. PTX was labeled with BIODIPY. ADR is autofluorescent. Cells were incubated with 100 nmol/L Mito-Tracker Green (30 min) and 10 μ mol/L Hoechst 33258 (15 min) to visualize mitochondria and nuclei, respectively. Then, cell monolayers were examined by confocal laser scanning microscopy (Zeiss LSM700, Germany).

P-gp expression assay

Cells were fixed with a 4% paraformaldehyde solution, followed by washing and blocking. Then, the cells were incubated with a FITC-conjugated anti-P-gp polyclonal antibody

or isotype-matched negative control for 1 h at 37°C. After washing, cells were analyzed for P-gp protein expression by flow cytometry (Beckman FC500, US).

Statistical analysis

All data are presented as the mean \pm SEM or mean \pm SD of at least three independent experiments. Statistical analyses included two-tailed Student's *t*-tests and one-way analysis of variances.

Results

SMI enhanced the inhibitory effects of ADR and PTX on tumor growth in LoVo colon cancer xenograft mice

The tumor volume was measured every two days to determine the influence of SMI on tumor development. At the endpoint (12 days after treatment), xenograft tumors were excised from mice in each group and photographed. Tumors in the SMI combination treatment group were smaller than in other groups (Figure 1A). However, SMI did not reduce the weight of mice (Figure 1B), indicating that SMI would not enhance the toxic effects of chemotherapeutics. The tumor weight/mouse weight ratio and volumes of SMI co-administered with the ADR or PTX group were significantly lower than those of groups treated with ADR or PTX alone (Figure 1D and 1C). Furthermore, as shown in Figure 1E, the tumor weight inhibition rate in SMI co-administered with ADR or PTX (34.6% and 37.6%, respectively) was markedly higher than that of the ADR alone or PTX alone (17.5% and 21.4%, respectively). Calculation of the tumor volume inhibition rate showed similar results (Figure 1F). In summary, SMI significantly increased the chemotherapy efficacy of ADR and PTX, whereas SMI itself had no obvious anti-cancer effect.

SMI enhanced the toxic effects of ADR and PTX on cancer cells in LoVo colon cancer xenograft mice

The effects of SMI on the toxicity of ADR and PTX in tumor tissues were histologically examined. Tumor necrosis was observed using HE staining. As shown in Figure 2A, the control and SMI groups presented with normal morphology and vigorous cell growth. By contrast, in the SMI-combination-treated group, a significant increase in necrosis and abnormal morphology was seen compared with the group treated with ADR or PTX mono-therapy. In addition, SMI did not increase the pathological damage induced by ADR or PTX on other important organs, such as the heart, liver and kidney (Figure S1). Immunohistochemical staining with the Ki67 antibody revealed that SMI combination treatment led to lower levels of Ki67 expression than either ADR or PTX mono-therapy (Figure 2B), indicating lower cell proliferation. In accordance with this result, the TUNEL assay showed that SMI significantly increased the effects of ADR and PTX on cancer cell apoptosis, which eventually inhibited tumor growth (Figure 2C).

SMI increased the ADR and PTX concentrations in plasma and tumor tissues

The SMI-combination-treated group was intraperitoneally

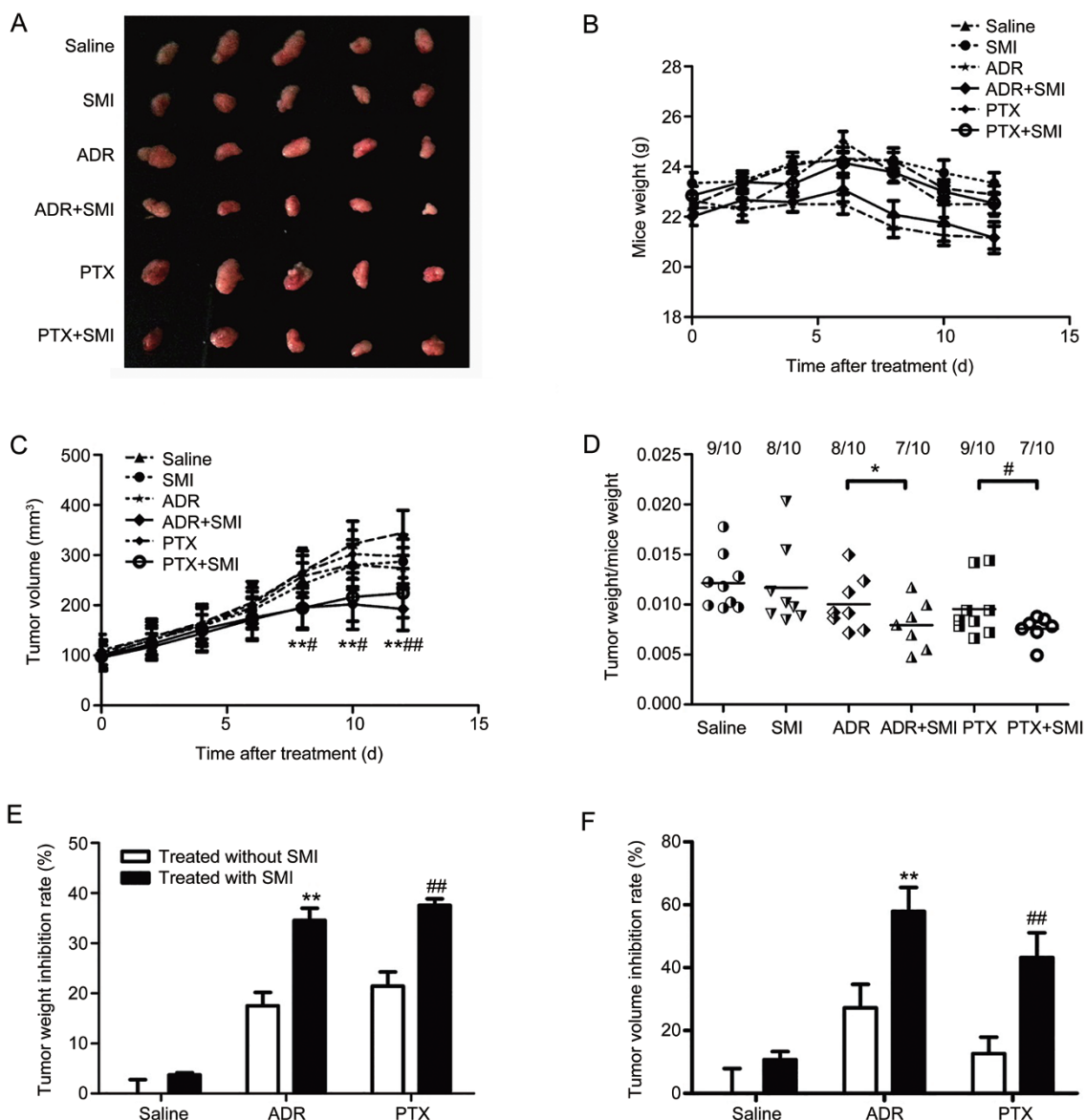


Figure 1. Synergistic effects of SMI with ADR and PTX in a LoVo colon cancer xenograft model. Mice were intraperitoneally injected with ADR (2 mg/kg, every three days) or PTX (7.5 mg/kg, every three days) with or without SMI (0.01 mL/g, every day) for 13 d. $n=7-10$. (A) Photographs of tumors from each group excised on d 13. (B) Mouse weight curve during treatment. (C) Tumor growth curve of each group during treatment. (D) The ratio of tumor weight and mouse weight in each group after the mice were sacrificed. (E) Tumor weight inhibition rate at d 13. (F) Tumor volume inhibition rate at d 13. * $P<0.05$, ** $P<0.01$ vs ADR treated groups. # $P<0.05$, ## $P<0.01$ vs the PTX treated group.

injected with SMI 30 min before the administration of chemotherapeutic agents. The drug concentrations in plasma from nude mice were determined at 10, 20, 40, 60, and 120 min after ADR or PTX administration. SMI increased the AUC_{0-2h} of ADR and PTX to 2.59-fold (75.2 ± 23.7 nmol/L·h vs 195.1 ± 32.5 nmol/L·h) and 1.16-fold (523.0 ± 49.7 nmol/L·h vs 608.9 ± 52.1 nmol/L·h), respectively, compared with that of mono-chemotherapeutics therapy (Figure 3A, 3B). The drug concentrations in tumor tissues were determined at 40 min, 1 h and 2 h. As shown in Figure 3C, the ADR concentrations in tumors at 40 min and 1 h increased by 1.89- and 1.30-fold, respectively, compared with those of mono-ADR therapy

(597.2 ± 41.7 vs 1131.4 ± 89.3 nmol/L and 471.1 ± 45.6 vs 609.1 ± 69.2 nmol/L, respectively). Additionally, the PTX concentration in tumor increased by 1.54- and 1.37-fold at 40 min and 1 h (171.3 ± 37.5 vs 263.4 ± 35.1 nmol/L and 361.5 ± 34.8 vs 458.6 ± 49.3 nmol/L, respectively) (Figure 3D). Nevertheless, at 120 min, no significant difference in the tumor drug concentration was observed between the SMI combined-therapy and mono-therapy groups. However, SMI did not increase the drug concentration in the heart, liver, spleen, lung, or kidney, as shown in Figure 3E-H, indicating that SMI did not enhance the toxic or side effects of ADR and PTX in these important organs.

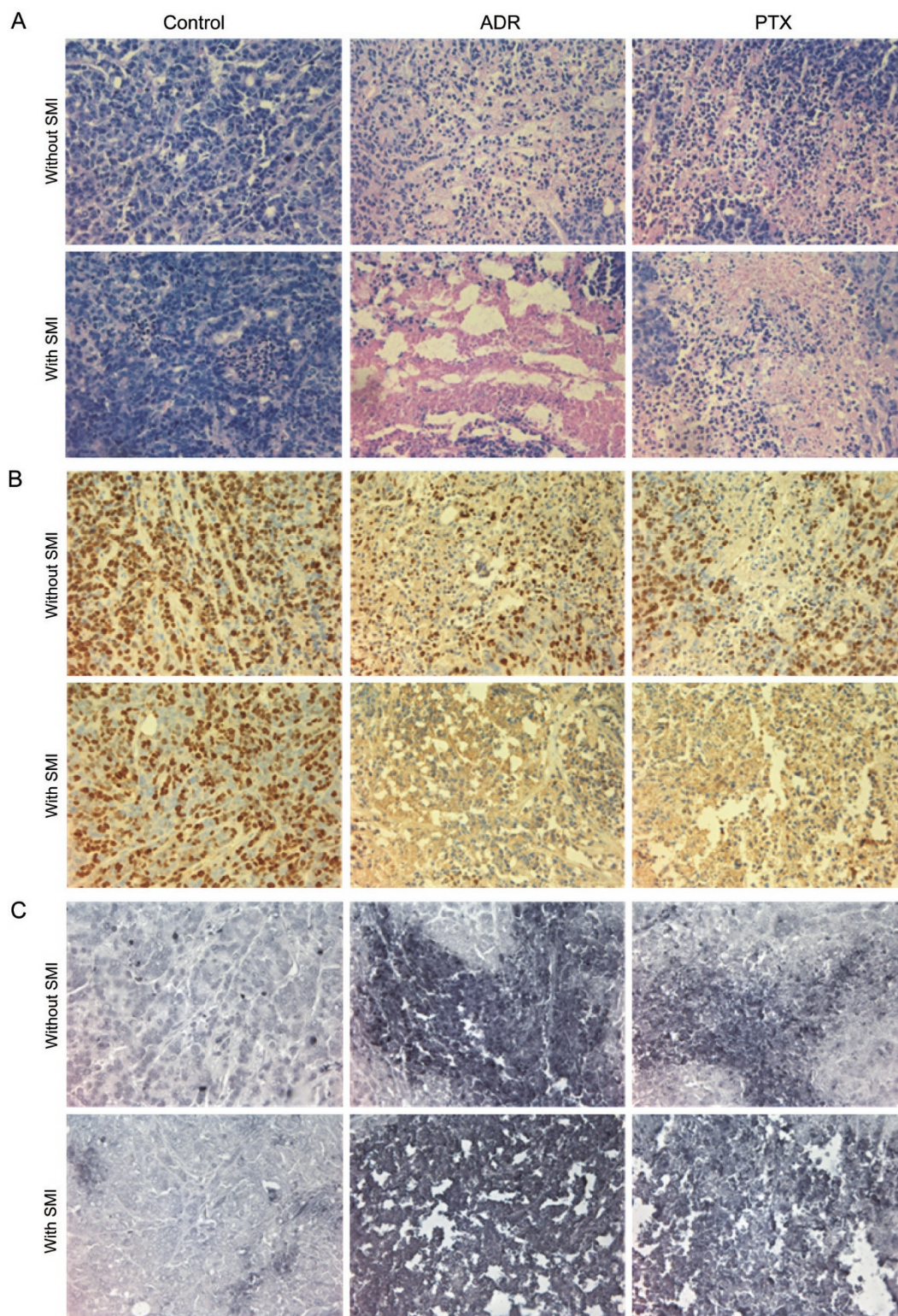


Figure 2. Effects of SMI combination treatment on the pathological histology of tumors in a LoVo colon cancer xenograft mice. (A) H&E staining of tumor tissues ($\times 400$). (B) Ki67 immunohistochemical staining of tumor tissues ($\times 400$). (C) TUNEL assay of apoptotic cells ($\times 400$). $n=6$.

SMI enhanced ADR- and PTX-induced growth inhibition and apoptosis in colon cancer cells

Based on the *in vivo* results, the chemosensitization effects

of SMI were further evaluated at the cellular level. First, the influence of SMI on the cytotoxic effect of chemotherapeutics was examined by MTT. As shown in Figure 4A–4D, both

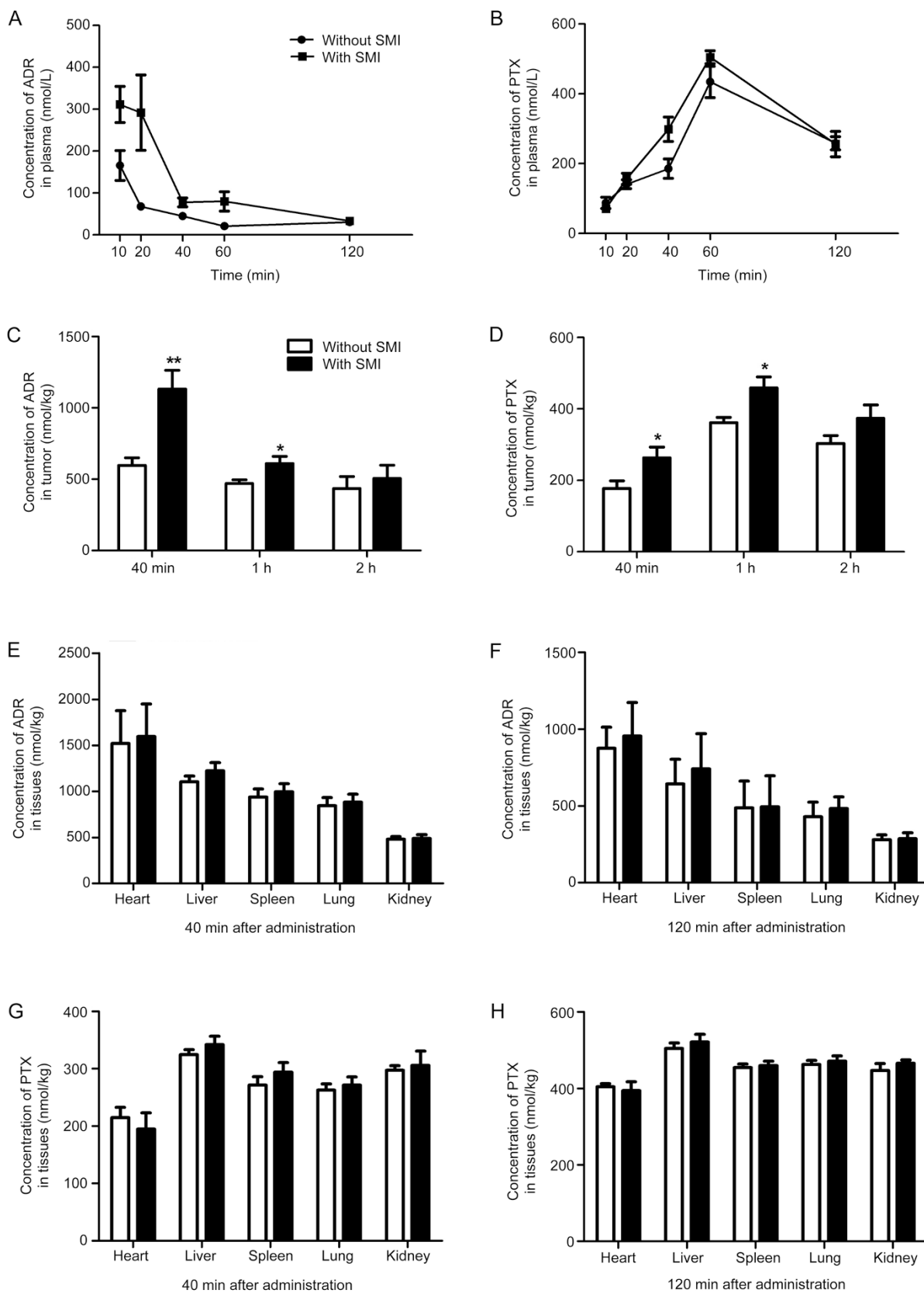


Figure 3. Effects of SMI on the ADR or PTX concentration in plasma, tumors, and non-malignant tissues of LoVo colon cancer xenograft mice. (A, B) Concentration-time curves of ADR or PTX in xenograft mice plasma. (C, D) Concentration of ADR or PTX in tumors. (E-H) Concentration of ADR or PTX in non-malignant tissues of xenograft mice. * $P < 0.05$, ** $P < 0.01$ vs without SMI. $n = 7-10$.

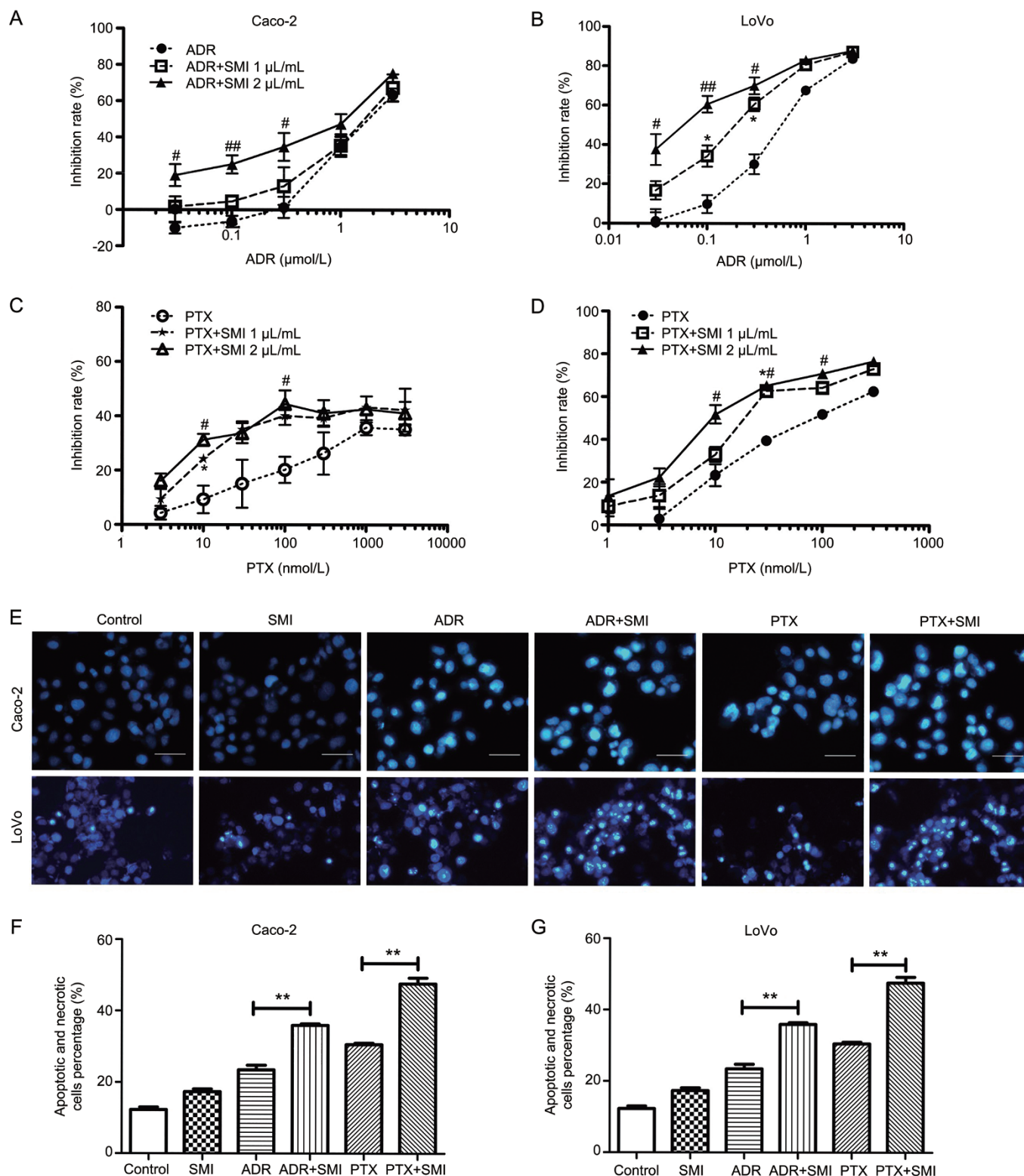


Figure 4. Effects of SMI on the cytotoxicity of ADR or PTX in colon cancer cells. Caco-2 and LoVo colon cancers were treated with ADR or PTX with or without SMI for 48 h. (A) Effects of SMI on the cytotoxicity of ADR to Caco-2 cells. (B) Effects of SMI on the cytotoxicity of ADR to LoVo cells. (C) Effects of SMI on the cytotoxicity of PTX to Caco-2 cells. (D) Effects of SMI on the cytotoxicity of PTX to LoVo cells. * $P < 0.05$, ** $P < 0.01$ between 1 $\mu\text{L/mL}$ of SMI co-treated group versus the group treated with chemotherapeutics alone. # $P < 0.05$, ## $P < 0.01$ between 2 $\mu\text{L/mL}$ of the SMI co-treated group versus the group treated with chemotherapeutics alone. (E) The effects of SMI on cell apoptosis induced by ADR or PTX. Colon cancer cells were incubated with ADR (500 nmol/L) or PTX (300 nmol/L) combined with or without SMI (2 $\mu\text{L/mL}$) for 24 h. Apoptosis was assessed using Hoechst 33258, and apoptotic features were assessed by observing the chromatin condensation and fragments staining ($\times 200$). Scale bar = 50 μm . (F, G) Detection of apoptotic and necrotic cells via flow cytometry. ** $P < 0.01$. Data are presented as the mean \pm SEM from five independent experiments.

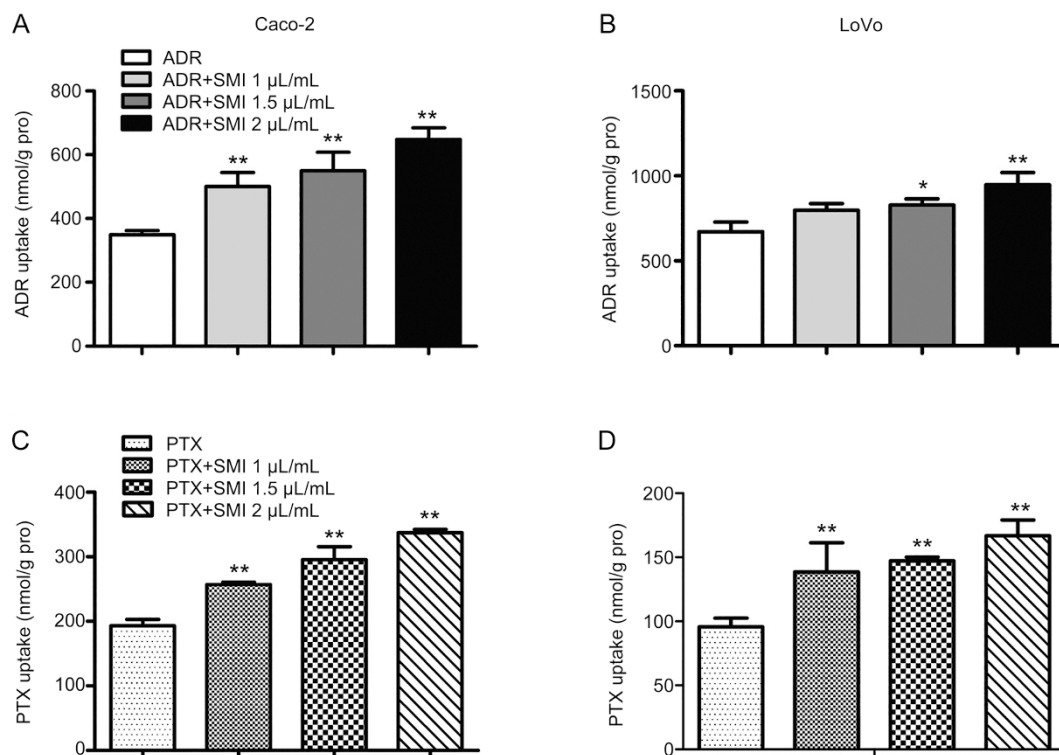


Figure 5. Effects of SMI on cellular accumulation of ADR or PTX in colon cancer cells. (A, B) Effects of SMI (1, 1.5, and 2 $\mu\text{L}/\text{mL}$) on cellular accumulation of ADR (5 $\mu\text{mol}/\text{L}$) in Caco-2 and LoVo cells. (C, D) Effects of SMI (1, 1.5, and 2 $\mu\text{L}/\text{mL}$) on cellular accumulation of PTX (5 $\mu\text{mol}/\text{L}$) in Caco-2 and LoVo cells. Data are presented as the mean \pm SD from five independent experiments. * P <0.05, ** P <0.01 vs the control group.

Caco-2 and LoVo cells co-treated with SMI and ADR (or PTX) were more sensitive to ADR or PTX alone. Treatment with SMI (1 or 2 $\mu\text{L}/\text{mL}$) for 24 h exhibited had little effect on the cell viability.

Hoechst 33258 staining was used to determine whether SMI affected ADR- or PTX-induced cell apoptosis. The nuclei of untreated and mono-SMI-treated colon cancer cells showed homogenous fluorescence with no evidence of segmentation or fragmentation. By contrast, segregation of cell nuclei into segments was apparent in cells incubated with ADR or PTX for 24 h, and co-administration of SMI intensified nuclear segmentation into dense nuclear parts as well as increased apoptotic bodies, as presented in Figure 4E–4G.

SMI increased the cellular accumulation of ADR and PTX in colon cancer cells

The accumulation of ADR and PTX in colon cancer cell lines was quantitatively examined by LC-MS/MS. The accumulation of ADR or PTX in Caco-2 and LoVo cells was increased in a SMI-concentration-dependent manner (Figure 5). This result was consistent with the results of a cytotoxicity assay.

The enhanced effect of SMI on the intracellular accumulation of ADR was positively correlated with the P-gp expression in colon cancer cells

Because both ADR and PTX are classic P-gp substrates, the changes in the intracellular accumulation with SMI may be

related to its impact on P-gp function. Here, the relationship between the intracellular accumulation of ADR and P-gp expression in four colon cancer cell lines was investigated. The fold change in the intracellular accumulation of ADR was closely correlated with the P-gp expression levels in four different cell lines ($r^2=0.8558$) (Figure 6C). Additionally, we calculated the correlation coefficients between the fold change in intracellular accumulation of the ADR and P-gp mRNA levels (Figure S2), and a similar result was obtained ($r^2=0.8404$). These results indicated that SMI might increase the intracellular drug concentration of ADR by hampering the efflux function of P-gp.

P-gp expression contributed to the chemosensitization effects of SMI on ADR and PTX

To further understand the relationship between the chemosensitization effect of SMI and P-gp, pharmacodynamic research was conducted on a MCF-7 human breast cancer cell line and its derivative P-gp-overexpressing MCF-7/ADR cells, which are resistant to ADR and PTX^[15]. The results demonstrated that SMI significantly increased the cytotoxicity of ADR or PTX in MCF-7/ADR cells. However, in MCF-7 cells, SMI failed to enhance the cytotoxic effects of ADR or PTX (Figure 7A–7D). In the meantime, SMI significantly increased ADR or PTX accumulation in MCF-7/ADR cells, but did not show any enhancement in the intracellular drug concentration in MCF-7 cells (Figure 7E, 7F).

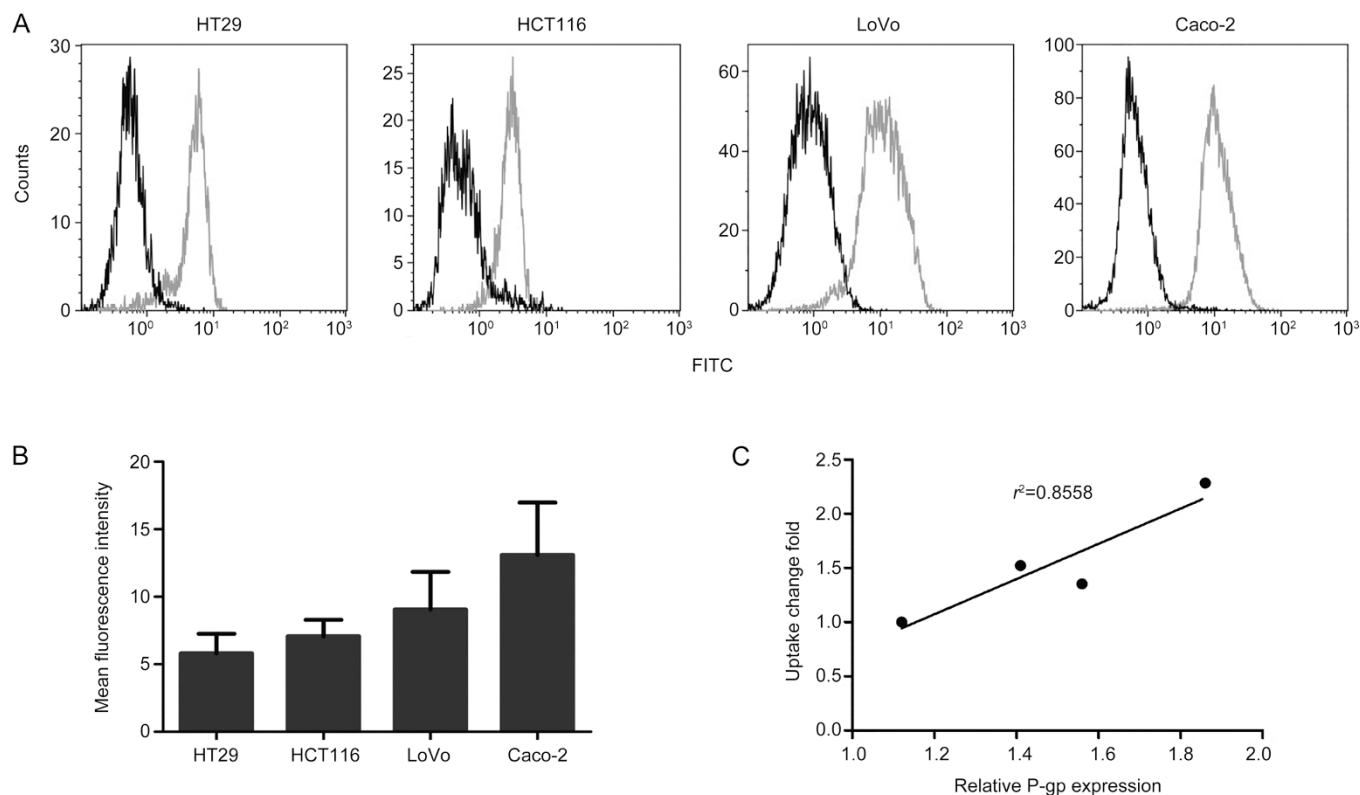


Figure 6. P-gp expression in four colon cancer cell lines and the correlation between SMI-induced changes in intracellular ADR accumulation and P-gp expression. (A) Detection of P-gp expression by flow cytometry. Green: FITC-P-gp and black: isotype control. (B) Mean fluorescence intensity of each cell line. (C) The correlation between SMI-induced changes in intracellular ADR accumulation and P-gp expression.

SMI increased the concentration of ADR or PTX in the target subcellular organelles

It is well known that ADR mainly accumulates in nuclei, binding DNA, and that PTX accumulates in the cytoplasm, binding microtubules. Therefore, the cytoplasm, mitochondria, and nuclei of colon cancer cells were separated for quantification of the ADR or PTX concentration. Additionally, fluorescence microscopy was used to evaluate ADR autofluorescence and BIODIPY-labeled PTX fluorescence. The ADR concentration in subcellular organelles is shown in Figure 8A–8D. SMI significantly increased ADR autofluorescence (red) in the nucleus (blue) and the ADR concentration in the nucleus by 2.6-fold in Caco-2 cells and 2.5-fold in LoVo cells. As shown in Figure 8E–8H, SMI significantly increased BIODIPY-labeled PTX fluorescence (red) around the nucleus (blue) and the PTX concentration in the cytoplasm increased by 1.6-fold in Caco-2 cells and 1.6-fold in LoVo cells. These results indicated that SMI improved the distribution of ADR and PTX in the target intracellular organelles, which might improve anti-tumor effects.

Discussion

The promise of Traditional Chinese medicine (TCM) in cancer treatment is increasingly being recognized, and TCM is one of the most common complementary therapies for chemotherapy, surgery, and radiotherapy used worldwide, especially in Asia. Shenmai injection (SMI) is derived from the famous

traditional Chinese herbal prescription Shendong yin, which invigorates Qi, nourishes Yin, and replenishes bodily fluids. Currently, SMI is a famous Chinese patent-protected injection that has been widely applied in clinical practice for treating shock with qi and yin deficiency, coronary heart disease, viral myocarditis and tumors^[4]. Various pharmacodynamic studies have demonstrated that SMI is effective in cancer interventions as an adjunct agent to chemotherapy^[4, 8, 16]. Shenmai was found to be effective in treating cancer-related fatigue and the side effects induced by chemotherapy or radiotherapy^[16], which can be explained by the synergistic effect of Shenmai for qi and yin. However, there is a lack of direct evidence to confirm the chemosensitization function of SMI or its underlying mechanisms. In this paper, the synergistic action of SMI in colorectal cancer was evaluated *in vivo* and *in vitro*. The underlying mechanism is explored from both a macro and micro perspective using pharmacokinetics.

Colorectal cancer is the third most common cancer and the third leading cause of cancer death in the world^[17]. It was demonstrated that intraperitoneal chemotherapy (5-fluorouracil combined with cisplatin) plus SMI is effective in treating post-operative patients with advanced colorectal cancer^[5]. However, no systemic basic research has been performed to elucidate the synergistic effects of SMI *in vivo* and *in vitro*. In the current study, the chemosensitization effects of SMI on two classical chemotherapeutic agents, ADR and PTX, were

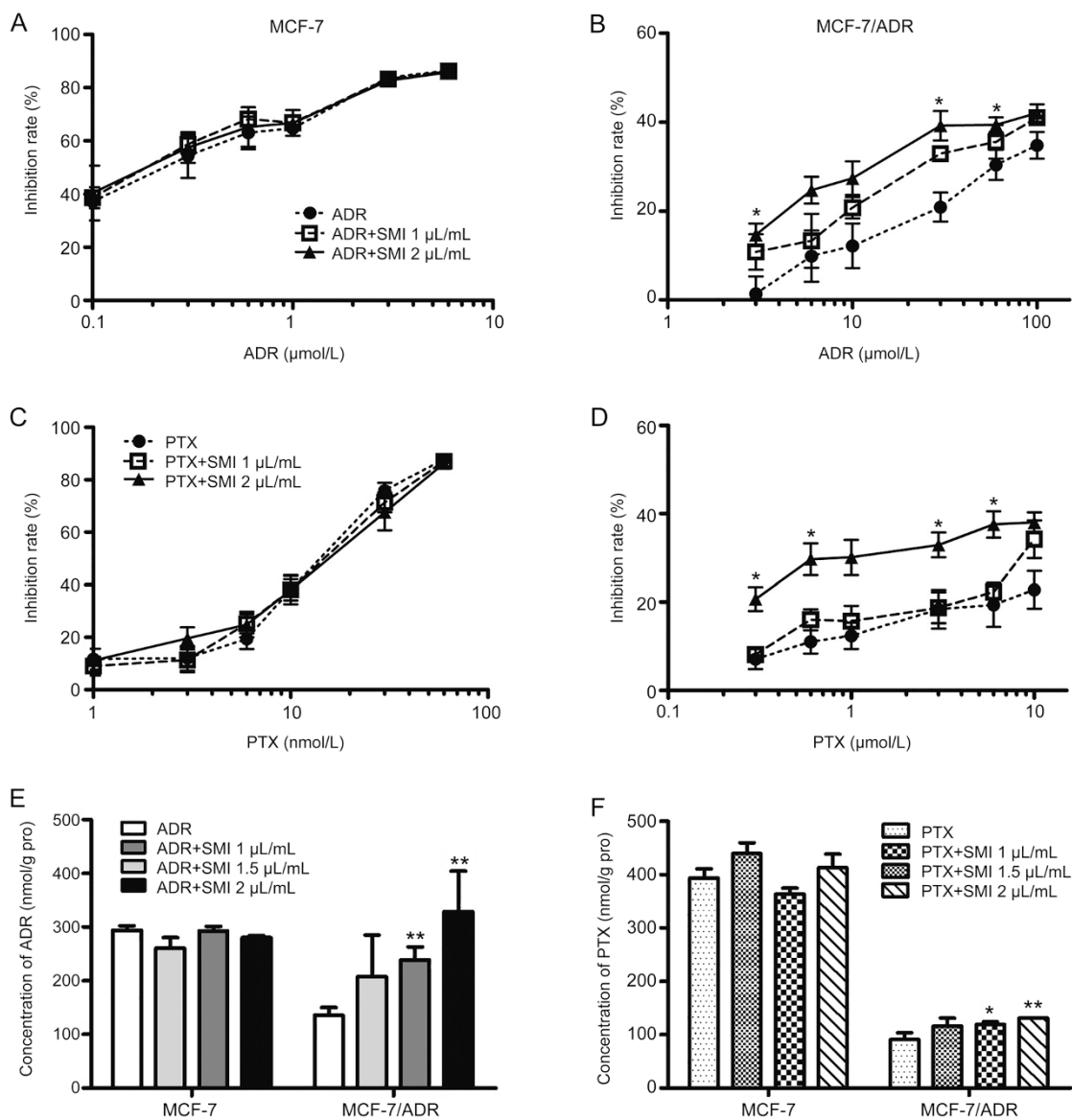


Figure 7. Influence of P-gp expression on the chemosensitization effect of SMI. (A–D) MTT assay. MCF-7 human breast cancer cells and derivative P-gp-overexpression MCF-7/ADR cells were treated with ADR or PTX combined with or without SMI (1 and 2 μL/mL) for 48 h. (E, F) Cellular accumulation of ADR or PTX. Breast cancer cells were treated with ADR or PTX with or without SMI for 2 h. Data are presented as the mean±SEM from five independent experiments. **P*<0.05, ***P*<0.01 vs the control group.

demonstrated in LoVo colon cancer xenograft mice (Figures 1 and 2) and in several cancer cell lines (Figures 4 and 7). Drug resistance and undesirable injury of other organs are the main factors that limit the clinical use of ADR and PTX. The present study also showed the synergistic effects of SMI and chemotherapeutic drugs without exacerbating ADR and PTX toxicity in non-tumor tissues, such as the heart, liver, spleen, lung, and kidney (Figure S1), which is supported by the ADR and PTX tissue distribution data in LoVo colon cancer xenograft mice. SMI had no significant impact on the ADR and PTX concentrations in the heart, liver and other tissues (Figure 3). In accordance with our results, SMI seems to be generally safe for clinical use^[4,6,8,18].

Many studies have found that the synergistic effects of SMI or its main components, ginseng saponins, with chemotherapeutic agents were due to the influence on multiple cancer signaling pathways, such as NF-κB, JNK, MAPK, p53, among others^[19,20]. However, few studies have explored the synergistic effects according to pharmacokinetics. To investigate whether the synergistic effects of SMI on ADR and PTX is related to pharmacokinetic changes, the ADR and PTX concentrations in plasma, tissues and tumor cells were detected by LC-MS/MS in the present study. Our results demonstrated that SMI significantly increased the AUCs of ADR and PTX as well as concentrations in the tumor tissues, but there was almost no change in the drug concentration in other important

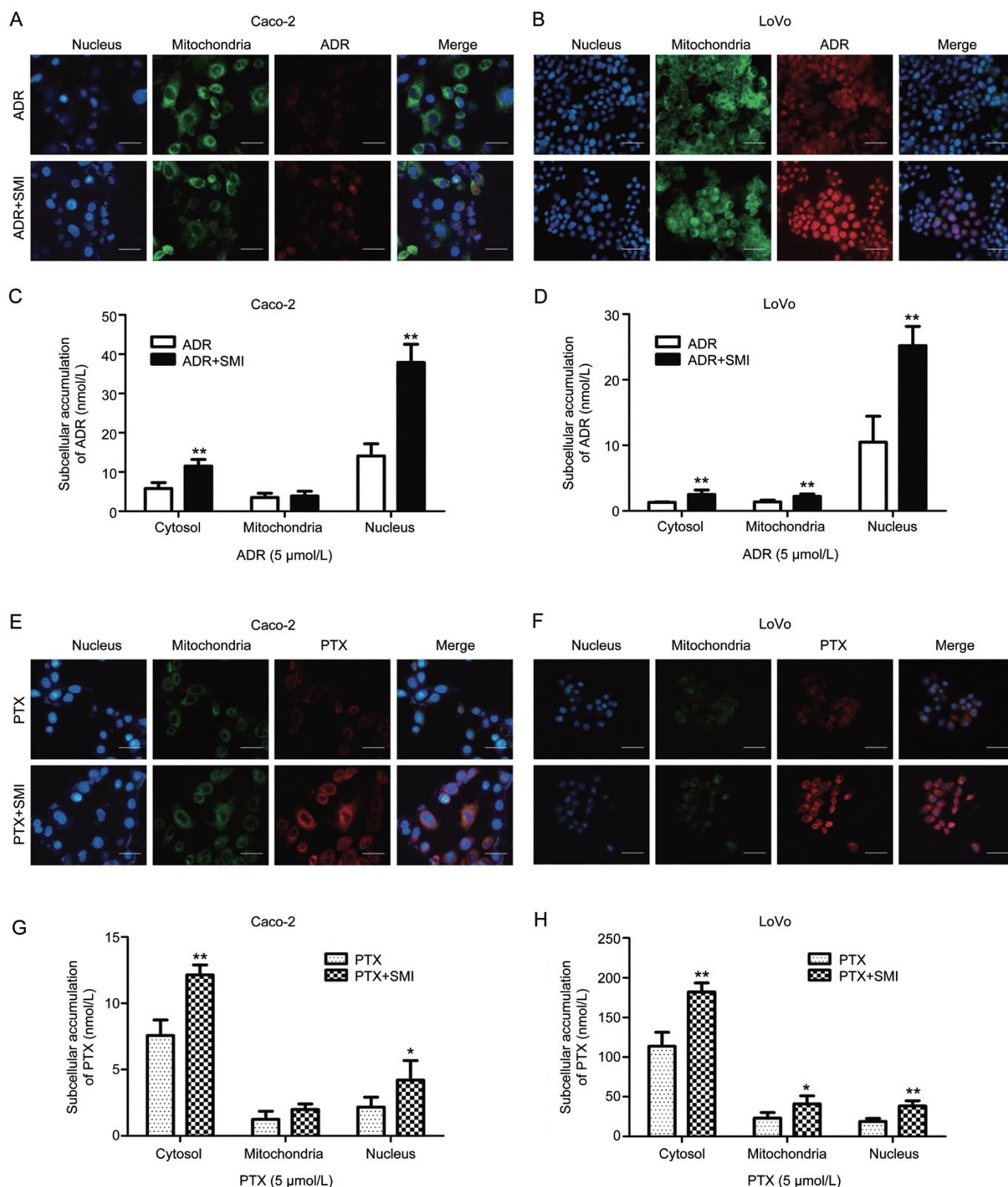


Figure 8. Effects of SMI on the subcellular distribution of ADR and PTX. Caco-2 or LoVo cells were treated with ADR or PTX combined with or without SMI (2 μL/mL) for 2 h. (A, B) Fluorescent images of ADR intracellular localization in Caco-2 or LoVo cells (×200). Scale bar=50 μm. (C, D) SMI effects on the subcellular distribution of ADR in Caco-2 or LoVo cells. (E, F) Fluorescent images of intracellular localization of BIODIPY-labeled PTX in Caco-2 or LoVo cells (×200). Scale bar=50 μm. (G, H) SMI effects on the subcellular distribution of PTX in Caco-2 or LoVo cells. Data are presented as the mean±SD from five independent experiments. * $P<0.05$, ** $P<0.01$ vs the control group.

organs (Figure 3). Similarly, SMI enhanced the ADR and PTX accumulation in Caco-2 and LoVo cells.

Ginsenoside Rh2 could inhibit P-gp-mediated efflux of chemotherapeutic drugs, increase the intracellular drug concentration and enhance the cytotoxicity of chemotherapeutic drugs^[15, 21]. P-gp functions as an ATP-driven transmembrane pump that can mediate the efflux of anti-cancer drugs^[22]. The present study also found that the synergistic effects of SMI were closely related to P-glycoprotein expression (Figures 6 and 7). Some of the ginsenoside constituents within SMI have an inhibitory effect on P-gp. As reported, 20(S)-ginsenoside F1 exhibited significant inhibition on P-gp in MDR1-MDCKII and Caco-2 cells^[23]. Three ginsenoside metabolites, CK, Ppd, and Ppt, significantly enhanced rhodamine 123 retention in Caco-2 cells and decreased the efflux ratio of digoxin; these effects were comparable to the effects of the known P-gp inhibitor verapamil^[24]. However, determination of the ingredients in SMI that play an important role in the chemosensitization effects requires further investigation.

After anti-cancer drugs are transported into cells, they are distributed to subcellular structures and eventually bind to their targets^[25]. Therefore, the cellular pharmacokinetic process of anti-cancer drugs in target cells is a determinant of its binding to the intracellular target, affecting its cytotoxicity^[26]. To improve our understanding of the action of SMI on the intracellular behavior of chemotherapeutic agents, the concentration of each drug concentration in subcellular organelles was determined. As shown in Figure 8, SMI significantly increased the ADR concentration in the nucleus and PTX concentration in the cytoplasm, which was also in accordance with the fluorescence image results. The different influence of SMI on the ADR and PTX concentrations in different subcellular organelles might be due to the different binding targets. These results indicated that SMI improved the distribution of chemotherapeutic drugs in cells, increasing the concentration of drugs in target organelles, which could facilitate better anti-tumor effects.

In summary, the current study demonstrated the direct synergistic effect of SMI both *in vivo* and *in vitro*, and the underlying mechanisms were studied based on pharmacokinetics. The current results provide direct scientific data for the use of SMI in clinical chemotherapy for colon cancers, which may guide combined drug regimens.

Abbreviation

Shenmai injection, SMI; adriamycin, ADR; paclitaxel, PTX; Traditional Chinese medicine, TCM; P-glycoprotein, P-gp.

Acknowledgements

The work is supported by the National Natural Science Foundation of China (No 81573496, 81530098, 81573494); Jiangsu Province Key Laboratory of Drug Metabolism and Pharmacokinetics Projects (No BM2012012); Natural Science Foundation of Jiangsu Province (No BK20131308, BK20160076); Open Research Fund of State Key Laboratory of Bioelectronics, Southeast University; China "Creation of New Drugs" Key

Technology Projects (No 2015ZX09501001); and Foundation for Innovative Research Groups of the National Natural Science Foundation of China (No 81421005).

Author contribution

Wen-yue LIU and Ji-chao HE performed most of the experiments and analyzed the data; Wen-yue LIU drafted the manuscript; Pin NI, Jia-li LIU, Qian-ying CHEN, and Qing-ran LI performed some of the experiments; Xiao-jie ZANG, Lan YAO, Ya-zhong LIU, Chao JIANG, Mu-lan WANG, and Pei-qiang SHEN assisted with the experiments; Guang-ji WANG, Fang ZHOU, Jing-wei ZHANG, and Xue-quan YAO designed the study; and Fang ZHOU reviewed the manuscript.

References

- 1 Liss AL, Abu-Isa EI, Jawad MS, Feng FY, Vance SM, Winfield RJ, et al. Combination therapy improves prostate cancer survival for patients with potentially lethal prostate cancer: the impact of Gleason pattern 5. *Brachytherapy* 2015; 14: 502–10.
- 2 Qi F, Zhao L, Zhou A, Zhang B, Li A, Wang Z, et al. The advantages of using traditional Chinese medicine as an adjunctive therapy in the whole course of cancer treatment instead of only terminal stage of cancer. *Biosci Trends* 2015; 9: 16–34.
- 3 Li J, Zhang F. The immunoregulatory effects of traditional Chinese medicine on treatment of asthma or asthmatic inflammation. *Am J Chin Med* 2015; 1–23.
- 4 Lu LY, Zheng GQ, Wang Y. An overview of systematic reviews of shenmai injection for healthcare. *Evid Based Complement Alternat Med* 2014; 2014: 840650.
- 5 Zhu WR, Zheng L, Guo YB, Yuan JM, Shen XH. Clinical research of intraperitoneal chemotherapy plus Shenmai Injection in treating advanced colorectal cancer. *Zhong Xi Yi Jie He Xue Bao* 2005; 3: 266–9.
- 6 Chen YZ, Li ZD, Gao F, Zhang Y, Sun H, Li PP. Effects of combined Chinese drugs and chemotherapy in treating advanced non-small cell lung cancer. *Chin J Integr Med* 2009; 15: 415–9.
- 7 Chen Z, Wang P, Huang WX, Liu LM. Experimental study on effects of shengmai injection: enhancing 5-FU anti-tumor efficacy and reducing its toxicity. *Zhong Xi Yi Jie He Xue Bao* 2005; 3: 476–9.
- 8 Wang L, Huang XE, Cao J. Clinical study on safety of cantharidin sodium and shenmai injection combined with chemotherapy in treating patients with breast cancer postoperatively. *Asian Pac J Cancer Prev* 2014; 15: 5597–600.
- 9 Dong QT, Zhang XD, Yu Z. Integrated Chinese and Western medical treatment on postoperative fatigue syndrome in patients with gastric cancer. *Zhongguo Zhong Xi Yi Jie He Za Zhi* 2010; 30: 1036–40.
- 10 Xia CH, Sun JG, Wang GJ, Shang LL, Zhang XX, Zhang R, et al. Herb-drug interactions: *in vivo* and *in vitro* effect of Shenmai injection, a herbal preparation, on the metabolic activities of hepatic cytochrome P450 3A1/2, 2C6, 1A2, and 2E1 in rats. *Planta Med* 2010; 76: 245–50.
- 11 Xia C, Sun J, Wang G, Shang L, Zhang X, Zhang R, et al. Differential effect of Shenmai injection, a herbal preparation, on the cytochrome P450 3A-mediated 1'-hydroxylation and 4-hydroxylation of midazolam. *Chem Biol Interact* 2009; 180: 440–8.
- 12 Zeng C, He F, Xia C, Zhang H, Xiong Y. Identification of the active components in Shenmai injection that differentially affect Cyp3a4-mediated 1'-hydroxylation and 4-hydroxylation of midazolam. *Drug Metab Dispos* 2013; 41: 785–90.

- 13 Zhang J, Zhou F, Wu X, Gu Y, Ai H, Zheng Y, *et al*. 20(S)-ginsenoside Rh2 noncompetitively inhibits P-glycoprotein *in vitro* and *in vivo*: a case for herb-drug interactions. *Drug Metab Dispos* 2010; 38: 2179–87.
- 14 Lu M, Zhou F, Hao K, Liu J, Chen Q, Ni P, *et al*. Alternation of adriamycin penetration kinetics in MCF-7 cells from 2D to 3D culture based on P-gp expression through the Chk2/p53/NF-kappaB pathway. *Biochem Pharmacol* 2015; 93: 210–20.
- 15 Zhang J, Zhou F, Wu X, Zhang X, Chen Y, Zha BS, *et al*. Cellular pharmacokinetic mechanisms of adriamycin resistance and its modulation by 20(S)-ginsenoside Rh2 in MCF-7/Adr cells. *Br J Pharmacol* 2012; 165: 120–34.
- 16 Lo LC, Chen CY, Chen ST, Chen HC, Lee TC, Chang CS. Therapeutic efficacy of traditional Chinese medicine, Shen-Mai San, in cancer patients undergoing chemotherapy or radiotherapy: study protocol for a randomized, double-blind, placebo-controlled trial. *Trials* 2012; 13: 232.
- 17 Siegel R, Desantis C, Jemal A. Colorectal cancer statistics. 2014. *CA Cancer J Clin* 2014; 64: 104–17.
- 18 Yu J, Xin YF, Gu LQ, Gao HY, Xia LJ, You ZQ, *et al*. One-month toxicokinetic study of SHENMAI injection in rats. *J Ethnopharmacol* 2014; 154: 391–9.
- 19 Gao JL, Lv GY, He BC, Zhang BQ, Zhang H, Wang N, *et al*. Ginseng saponin metabolite 20(S)-protopanaxadiol inhibits tumor growth by targeting multiple cancer signaling pathways. *Oncol Rep* 2013; 30: 292–8.
- 20 Zhang F, Li M, Wu X, Hu Y, Cao Y, Wang X, *et al*. 20(S)-ginsenoside Rg3 promotes senescence and apoptosis in gallbladder cancer cells via the p53 pathway. *Drug Des Devel Ther* 2015; 9: 3969–87.
- 21 Zhang H, Gong J, Kong D. Induction of apoptosis and reversal of permeability glycoprotein-mediated multidrug resistance of MCF-7/ADM by ginsenoside Rh2. *Int J Clin Exp Pathol* 2015; 8: 4444–56.
- 22 Paolini A, Baldassarre A, Del Gaudio I, Masotti A. Structural features of the ATP-binding cassette (ABC) transporter ABCA3. *Int J Mol Sci* 2015; 16: 19631–44.
- 23 Li X, Hu J, Wang B, Sheng L, Liu Z, Yang S, *et al*. Inhibitory effects of herbal constituents on P-glycoprotein *in vitro* and *in vivo*: herb-drug interactions mediated via P-gp. *Toxicol Appl Pharmacol* 2014; 275: 163–75.
- 24 Li N, Wang D, Ge G, Wang X, Liu Y, Yang L. Ginsenoside metabolites inhibit P-glycoprotein *in vitro* and *in situ* using three absorption models. *Planta Med* 2014; 80: 290–6.
- 25 Bhirde AA, Kapoor A, Liu G, Iglesias-Bartolome R, Jin A, Zhang G, *et al*. Nuclear mapping of nanodrug delivery systems in dynamic cellular environments. *ACS Nano* 2012; 6: 4966–72.
- 26 Zhou F, Zhang J, Li P, Niu F, Wu X, Wang G, *et al*. Toward a new age of cellular pharmacokinetics in drug discovery. *Drug Metab Rev* 2011; 43: 335–45.